Design Improvement of Transcatheter Aortic Valves for Aortic Stenosis Patients

Samantha K. Shoun[1], Ali N. Azadani[2]
[1]Student Contributor, University of Denver
[2]Advisor, Department of Mechanical and Materials Engineering, University of Denver

Abstract

Aortic valve disease is a common condition in patients above 60 years of age and is associated with significant morbidity and mortality. Aortic valve stenosis is characterized by the narrowing of the aortic valve, which can be quite debilitating. This disease is treated with transcatheter aortic valve replacement (TAVR), which is a rapidly expanding alternative to open-heart surgical aortic valve replacement (SAVR). Although TAVR is a less invasive than SAVR, long-term durability of the transcatheter aortic valves could be the Achilles heel of the procedure. Thus, the main objective of this research was to improve the design of transcatheter aortic valves using experimental testing and design analysis. After the design, building, and testing phases of four differing valves, it was seen that there are benefits to two specific designs. One design was a TAV based on a native aortic valve while the other was a TAV geometry that was optimized by finite element modeling. The native valve performed well during diastole based on its average regurgitation volume, while the optimized valve performed well during systole based on its average positive pressure difference and effective orifice area.

Keywords: Transcatheter aortic valve replacement, aortic valve, heart, experimental testing, 3D printing, laser cutting, stent, Dacron, leaflets, SolidWorks

1 INTRODUCTION

Aortic stenosis, which is caused by a calcific aortic valve disease, is currently the main cause for aortic valve replacement in developed countries[1]. Aortic valve stenosis affects 2–7% of the population above 60 years of age and projections indicate AS prevalence will triple by 2050, due to the aging population[1;2;3;4;5]. TAVR has emerged as a safe and effective alternative to SAVR for the treatment of patients with symptomatic severe aortic stenosis[6;7;8;9]. In TAVR, a transcatheter aortic valve (TAV), made from biological tissue, is folded up on a catheter, passed through an artery into the heart, and expanded within the calcified native aortic valve (Figure 1)[10]. The native valve is the natural biological valve within a heart. TAVR is a non-invasive procedure, and the recovery time is substantially shorter than SAVR. However, durability is the Achilles heel of TAVs[11;12;13;14;15]. Dvir and colleagues[12] estimated structural valve degeneration rate of TAVs to be approximately 50% at 8 years. The rate of structural valve degeneration in *surgical bioprosthetic valves* is known to be less than 15% at 10 years[16]. To be able to expand TAVR effectively to patients with a long-life expectancy, long-term durability of a TAV should match with that of a surgical bio prosthesis (SAV).

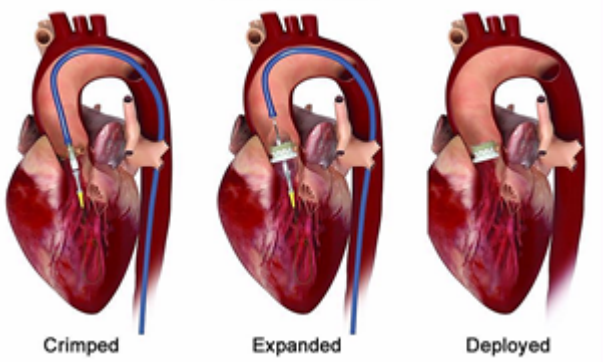

Figure 1. TAVR Procedure. A crimped valve is put in the aortic position using a catheter. Picture taken from Antelope Valley Hospital[10].

Researchers have focused on the understanding of the structural mechanics of TAVs to improve longevity with SolidWorks modeling and simulations. The valves consist of three main components. Firstly, there are the leaflets, which make up the main part of the valve. Three of these mirrors each other in an arranged cylin-

drical fashion to allow blood flow to seamlessly pass through the valve. The leaflets are generally made of bovine, or porcine pericardial tissues[14;15]. Next is the stent, which is a cylindrical frame with high radial strength to hold the valve in place. This provides a sturdy containment vessel for the leaflets. Generally, these stents are crafted with a tough but expandable material, such as cobalt chromium, stainless steel, and nitinol[12]. Strong yet pliable material is required due to the harsh and ever moving cardiac environment. The final component is a piece (or two) of Dacron fabric, which is used as an anchor to attach the leaflets to the stent, and block areas which could cause leakage or regurgitation. All parts of a completed valve can be seen in the labeled image (Figure 2). It is widely accepted that high stress regions initiate calcification by damaging the structural integrity of fixed tissue[17]. These regions must be minimized through design.

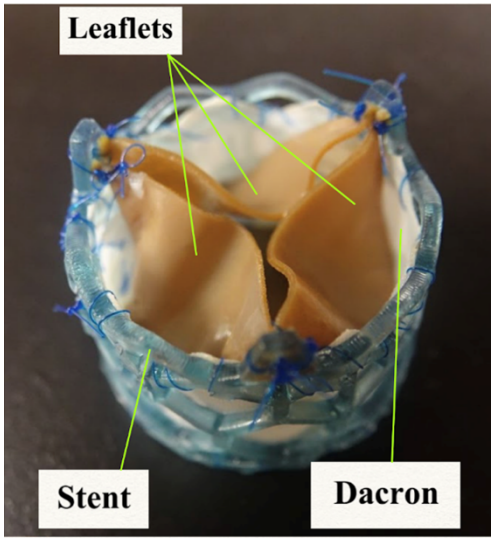

Figure 2. Labeled image of finished TAV including all three components: 1) Leaflets, 2) Stent, 3) Dacron. The TAV was built at the University of Denver by Samantha Shoun.

Valve designs require specific geometries and ratios to safely simulate real heart valves[18]. A successful design has been produced by Sapien 3[19]. In the past few years, a few computational frameworks have been developed to optimize TAV leaflet geometry and minimize peak stress on the leaflets[20]. Researchers at the DU Cardiovascular Biomechanics Lab recently optimized TAV leaflet geometry using computational simulations[20]. The optimized leaflet geometry was compared with a commercially available TAV (Edwards SAPIEN 3). A considerable reduction in the maximum in-plane principal stress was observed in the optimized leaflet geometry compared to Sapien 3 (Figure 3). The optimization results underline the opportunity to improve leaflet design in the next generation of TAVs to potentially increase long-term durability. A limitation associated with these studies was that the effect of TAV leaflet geometry was not studied on the valve hemodynamics (blood flow motion). Moreover, it is not clear to what extent structural and hemodynamic performance of the optimized valve geometry are like that of a native aortic valve. TAVs typically have a vertical non-expanding post in contrast to a contoured shape of native valve.

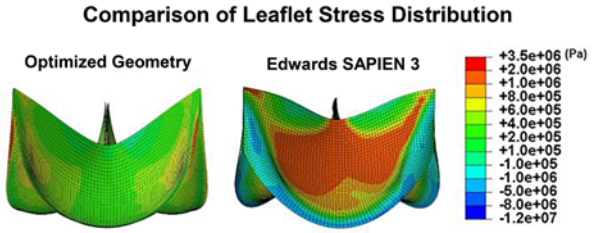

Figure 3. A considerable reduction in the peak in-plane maximum principal stress was observed in the optimized TAV geometry in comparison to the commercially available SAPIEN 3 valve[20]

.

In this study, four transcatheter aortic valves will be designed, built, tested, and analyzed with the goal of creating durable and effective TAV designs for a TAVR procedure. Three optimized valves will be created, with designs based on geometry that has been optimized by finite element modeling. Ideal valves will have little to no regurgitation volume, a low PPD mean, a high effective orifice area, and small variance within all data sets. Changes in these data will tell the researchers which valve designs are preferrable. Another additional valve will be created based upon the (average) native valve geometry and will serve as a control. All valves will have a 26 mm diameter to best simulate a TAV that would be used in a real life TAVR procedure. It is hypothesized that the final iteration of the optimized design will perform better than the first optimized iterations and the native design.

2 METHODS

2.1 Designing the Optimized and Native Transcatheter Aortic Valves

A statistically averaged geometry of a healthy aortic valve was created in SolidWorks based on reported values in the literature[18] (Figure 4). This was a framework for the designs of the transcatheter aortic valves. As in several different experiments[21], valve designs were created based upon ratios of general aortic valve geometries. These ratios are represented by certain valve lengths and angles (Figure 5). With set ratios of 1.2 for R_b/R_c and 1.4 for H/R_c, values for both the optimized and native designs were calculated. The optimized valves had a R_b of 13 mm, a decided height of 15.17 mm, and a commissure radius of 10.83 mm. In addition, the optimized model had a α of 23.58° and a θ

of 25.308°. These values differed from that of the native design in order to provide a better geometry based on finite element modeling for the man-made valve. The native valve measurements were 14.6 mm for height, 12.5 mm for R_b, 12.5 for R_c, 20° for α, and 34° for θ. The optimized valve had different radii for the commissure/base regions, while the native design required the same radii for both regions. The next step was to design the leaflets on SolidWorks. Two circles representing the base and commissure region were projected with a distance between them equal to the height of the perspective valves. The circles were cleaved into six even sections, each which would contain one half of a leaflet. A small space was added between the areas where each leaflet began and ended. This prevented overlap. Lines pertaining to the angles listed above were added as a blueprint for the leaflets. The spline function of SolidWorks was utilized to create the free edge and bottom boundary edge of each leaflet. Several points were carefully placed along blueprint lines to guide the spline. The area contained between the splines was filled then duplicated in a circular fashion to create three identical leaflets. Each one fell within the cleaved regions. Lastly the SolidWorks flatten function was able to flatten each leaflet into a 2D model that could be used as a template in the building portion of the experiment.

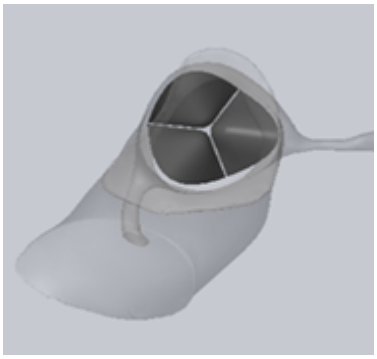

Figure 4. Statistically averaged geometry of a healthy aortic valve (top view).

With the leaflets completed, the Dacron and stent could be designed on SolidWorks as well. The stent is a crucial aspect of the valve, and it is generally designed to withstand the dynamic environment of a heart[21]. The prototypes in this experiment were 3D printed frames, since the focus was on the action of the leaflets and the basic geometry of the stents. The frame was not crimped, or balloon expanded. The stents were designed to be taller than the valves to fully encapsulate and protect the inner valve components[19] and were designed to have a thickness of 1 mm. The additional height added to the stent was one third of the original leaflet height. The first design of the stents was inspired by the Sapien 3 valves[19]. The repeating geometric pattern of a TAV stent is utilized to secure the

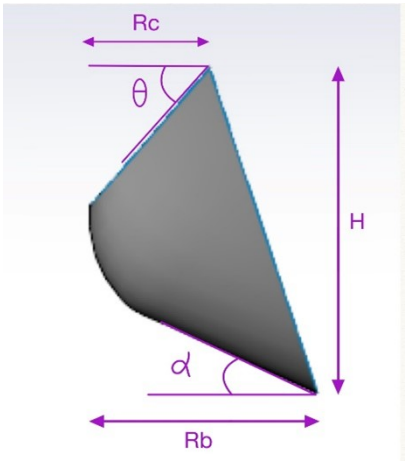

Figure 5. The ratios of valve properties are based upon differing geometries of both the leaflets and surrounding stent. The perspective shown is the side view of one leaflet. Defined valve parameters: R_b: radius at base; R_c: radius at commissures; θ: angle of free edge to the horizontal; H: leaflet height; α: angle from the base to the bottom valve edge

leaflets and assist with expansion and constriction of the valve during the TAVR procedure. The prototypes in this experiment still focused on a design that could be balloon expanded in future experiments using a different material. This was crafted on SolidWorks by first sketching a section of the geometric stent pattern then repeating for a total length that would equal the circumference of the valve. Next, the Dacron was fashioned to tightly fit into this stent. It was also inspired by the Sapien 3 valves[19]. The top portion of the Dacron fabric included the same geometric pattern as the top area of the stent. This allowed for the Dacron to align perfectly with the stent. The edges of the Dacron were created at an angle to later aid in the suturing and attachment of the components. As the experiment continued these same methods were used with altered designs to produce all the prototype valves. The outcome was several SolidWorks designs for each valve iteration (Table 1).

2.2 Building the Optimized and Native Transcatheter Aortic Valves

In the DU Cardiovascular Biomechanics Lab, three TAVs were constructed based on the optimized valve geometry[20], and one additional TAV was built based on a native design. Each valve was designed and created following the testing of the prior valve. This allowed for each iteration to improve upon the previous version. The building of these valves required two main pieces of hardware, including an Epilog Fusion M2 laser cutter[22] and Formlabs Form 2 resin printer[23]. The laser cutter resides in the DU Innovation Center while the 3D resin printer is in the mechanics shop at DU. To begin, the file for each flattened leaflet was

uploaded to the laser cutter from SolidWorks. Three identical leaflets were cut out of Edwards Lifesciences bovine pericardium. It was crucial to create a phosphate buffered normal saline solution[24] to store the leaflets in once they were removed from the main sheet of pericardium. This kept them moist and viable for testing. Proper cleaning techniques were in place to ensure the laser cutter would not be contaminated. The designs for the outer, and later inner Dacrons were cut from the laser cutter as well. This allowed for these small designs to be cut precisely. However, a small border equaling the diameter of the laser was added to each design as a tolerance to avoid cutting down the original size. The stent designs involved some trial and error in the building process. The stents were initially printed using a plastic filament; however, they were far too weak to survive soaking in the saline and testing. The filament broke down in the fluid. This was when the resin printer was utilized. A tough photopolymer resin was used to create the stents (Table 1). Each precise layer was added until the stent was fully printed, then the final product was washed in alcohol and water for safe handling. The stents were then placed under a UV light to harden.

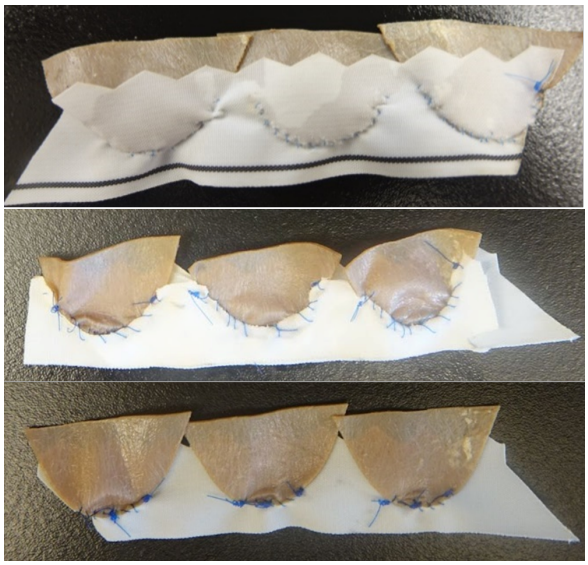

Figure 6. Running suture technique to secure the leaflets to the Dacron fabric.

With all necessary components, the valves were prepared for assembly. The first step of assembly was to suture the leaflets to the outer Dacron and later to the inner Dacron as well. A running suture was used in the last three valves (Figure 6). It was often helpful to place a few singular sutures along points to fasten the leaflets before the suturing. Once the leaflets were secured between the Dacron pieces, the edges were sewn together. Each Dacron piece was sewn separately. This produced a cylindrical Dacron/ leaflet sheet with the leaflets facing inward. Next, the Dacron was tightly sewn to the stent. The stent was cut from its resin supports using a scalpel to prepare for sewing. Using a running suture method, the bottom part of the Dacron was secured to the posterior end of the stent. The middle and top sections were then attached. It was important to line up the geometry of the Dacron with that of the stent to ensure the height of the leaflets was correct. A Mitutoyo Digital caliper was used to ensure that the height was the same as the SolidWorks design. Once fully secured, the tips of the leaflets were sewn to the commissure posts with three stitches on each end. There were three posts per stent, each with an angle matching that of the TAVs free edge (θ). This completed the assembly of the valves. Each valve appeared similar with a few key improvements and modifications (Table 1). To prepare for testing, the valves were tightly wrapped in a white covering and placed in a ring to secure their place in the pulse duplicator.

2.3 Testing the Optimized and Native Transcatheter Aortic Valves

The final step was to test the valves in an in vitro pulse duplicator (Figure 7). A pulse duplicator system simulates a cardiovascular environment. It analyzes the valves under dynamic physiological loading conditions[24]. The input parameters of the pulse duplicator complied with the international standard ISO 5840: 2015 recommendations for testing prosthetic heart valves[24]. These standards included a heart rate of 70 beats/min, a cardiac output of 5 L/min, a mean atrial pressure of 10 mmHg, and a mean aortic pressure of 100 mmHg[24]. As mentioned previously, the valves were prepared in a cylindrical disc and placed in the aorta section of the pulse duplicator (Figure 7). A solution of glycerin and saline was loaded in various chambers of the pulse duplicator to simulate the viscosity of blood. A solution of 37% glycerin and 63% saline proved to be the best substitute for the blood. The pulse duplicator had a flowmeter attachment to assist in measuring the systolic and diastolic cycles of the "blood" flow. The physiological flow condition of a heart was simulated through the manipulation of peripheral resistance and local compliance in the pulse duplicator system[24]. Once the valve was placed in the artificial heart attachment, it was submerged into a tank of water then sealed off. The tank was pumped with more water to ensure the calculated pressure differences would be accurate. No air was left in the tank. After the flowmeter was calibrated, the duplicator recirculated the glycerin/saline solution through the device apparatus and artificial heart. Strain gage pressure transducers were used to measure the pressure on the aorta and left ventricle areas of the pulse duplicator apparatus[24]. The pulse data was recorded on an in-lab personal computer, and was ready for later analysis.

Optimized Valve #1	*Optimized Valve #2*	*Optimized Valve #3*	*Native Valve*
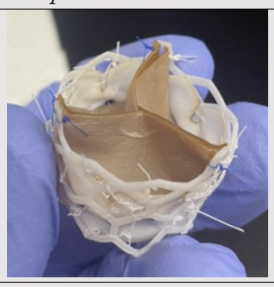			
SolidWorks Designs			
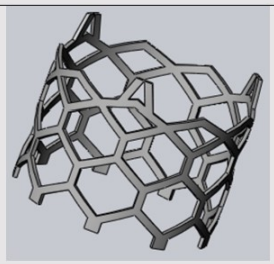		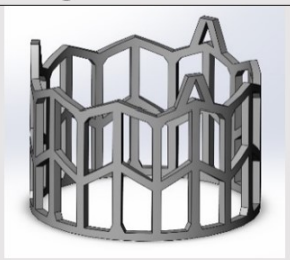	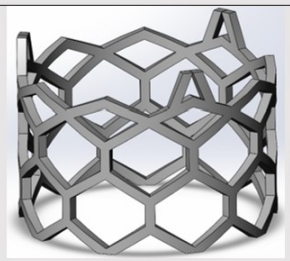
Optimized Leaflets		*Native Leaflets*	
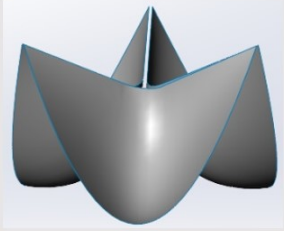	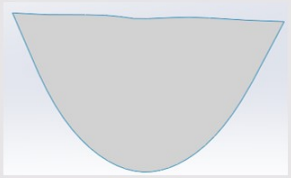	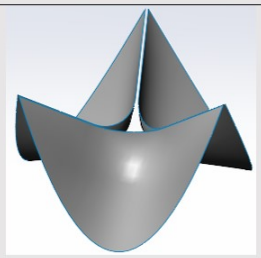	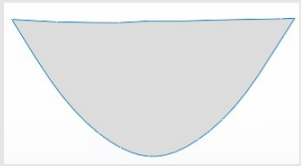

Table 1 Each valve iteration improved upon the next as seen in the final products and the SolidWorks designs. The optimized valves used the same leaflet design, while the leaflet design for the native valve was different. White stent = weaker plastic filament; Blue stent = stronger resin material.

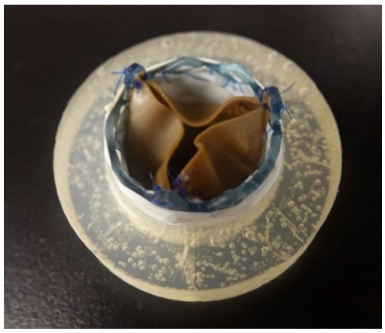

Figure 7. Left – DU pulse duplicator system; Right – valve prepped for testing in a washer to be mounted in the pulse duplicator.

3 RESULTS

During the pulse duplicator tests, each complete systolic and diastolic cycle was represented by real time inputs for the aortic region of the prosthetic heart, the ventricular region, and the overall flow (Figure 8). These produced a continually changing output of graphs for each valve iteration (Figure 9). With these figures, there was also an output of thousands of supplementary data points for the time during the test, flow levels, and pressures. These data were evaluated in excel to calculate a total regurgitation volume, effective orifice area, root mean square flow (RMS F. Flow) from the start of the forward flow to the end of the forward flow, and a mean positive pressure difference (PPD Mean)[25]. All values were calculated from a PD-100 System User Guide provided by BDC Laboratories[25]. These values were calculated for the first optimized valve, the sec-

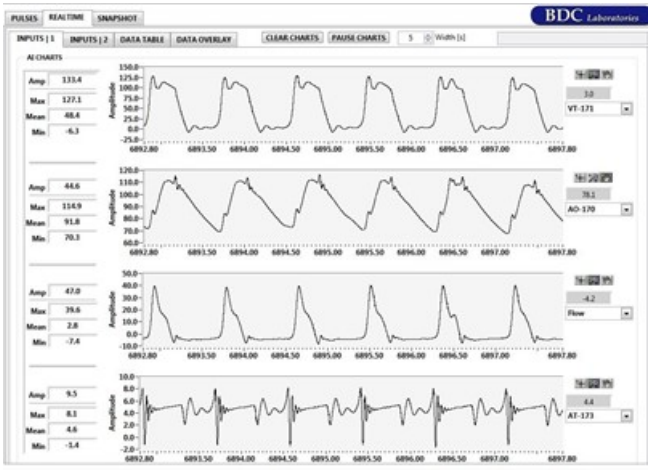

Figure 8. General real time graphs recorded during pulse duplicator tests. Represent regions of dynamic changes in prosthetic heart. The first curve represents the LV pressure, the second represents the aortic pressure, third shows the flow, and fourth demonstrates the left atrium pressure.

ond optimized valve, and the native valve (Table 2). The flow cycles were recorded incorrectly for the third optimized design, making the results void. However, the mean pressure gradient as well as the regurgitation volume for the third optimized design were approximated to be about the same as the values obtained for the second optimized valve.

4 DISCUSSION

This experiment proved to be successful. The first optimized valve was based upon prior research from the University of Denver and other various research institutions, as mentioned. The key differences from the first optimized valve to the second were the addition of an adjacent inner Dacron piece, a differing suture, and an improved stent. The inner Dacron piece allowed for a watertight seal around the inner portion of the valve that prevented leaking and regurgitation. The top portion of the inner Dacron piece was designed to outline the free edge of each leaflet, differing from the outer Dacron piece (Figure 10). Next, it was decided that a continuous running suture would be used to prevent holes in the prototypes as well (Figure 6). The first optimized valve had single sutures lining the areas of connection, however, several other experiments show that continuous sutures are preferred[26]. Continuous sutures allow for tighter seals. Finally, the stent was modified to aid in the suturing process and better contain the valve. The evolution of the stent is demonstrated in the visual attached (Table 1).

Several changes were made to the valve designs throughout the experimental process. The first two optimized valves had some issues staying in place as they were being tested, prompting the researchers to wrap the native valve as well as the following two optimized valves in white covering before testing. From the second valve to the third, the sutures were placed closer together and in higher quantity to secure the components of the valve further. The continuous suture technique was still utilized. Furthermore, it was decided to lengthen the leaflets. This allowed for the original design of each leaflet to remain unchanged during the suturing process by providing a border for the sutures around each leaflet. While this aided the design of the third optimized valve, it hurt the fourth. The leaflets became too long and protruded out of the top of the stent (Table 1). The third optimized valve also had issues with the cycle recording during testing. There was a calibration error with the flowmeter, which compromised the data (Figure 9). The zero for the flow cycles was calibrated incorrectly. This led to the researchers not being able to differentiate between the cycles for the third optimized valve which made it impossible to calculate quantitative values for this valve. However, the PPD mean and regurgitation values for the third optimized valve can be estimated to be the same as these values for the second optimized valve.

It was hypothesized that the final iteration of the optimized design would perform better than the first optimized iterations and the native design. The hypothesis was supported by the results of the second optimized valve but partially rejected by the results of the native valve. The native valve performed better than all tested valves during diastole, however the second iteration of the optimized valve performed better during systole. A systolic analysis is often more crucial than a diastolic analysis, the cycle patterns for each are seen in (Figure 11). As seen in Table 2 specific values for each valve were calculated on excel. To explain what is being seen in Table 2, the PPD mean pressure is the positive pressure difference between cycles. The RMS F. Flow represents the root mean square forward flow from forward flow start to forward flow end when the flow transitions from positive to negative. The effective orifice area is the minimal cross-sectional area of the flow[27]. Finally, the total regurgitation volume is the volume of fluid that enters back through the valve after systole and during diastole. If this number is too high, it could cause serious health issues for a patient. As previously stated, an ideal valve would have little to no regurgitation volume, a low PPD mean, a high effective orifice area, and small variance in the data sets. The variance can be evaluated by looking at the standard deviation of each data set (Table 2). A lower standard deviation is preferable.

The valves can be compared in systole based on their pressure gradient as well as in diastole based on their regurgitation. The optimized geometry provides support for the hypothesis through the analysis of the systole conditions. The second optimized geometry had

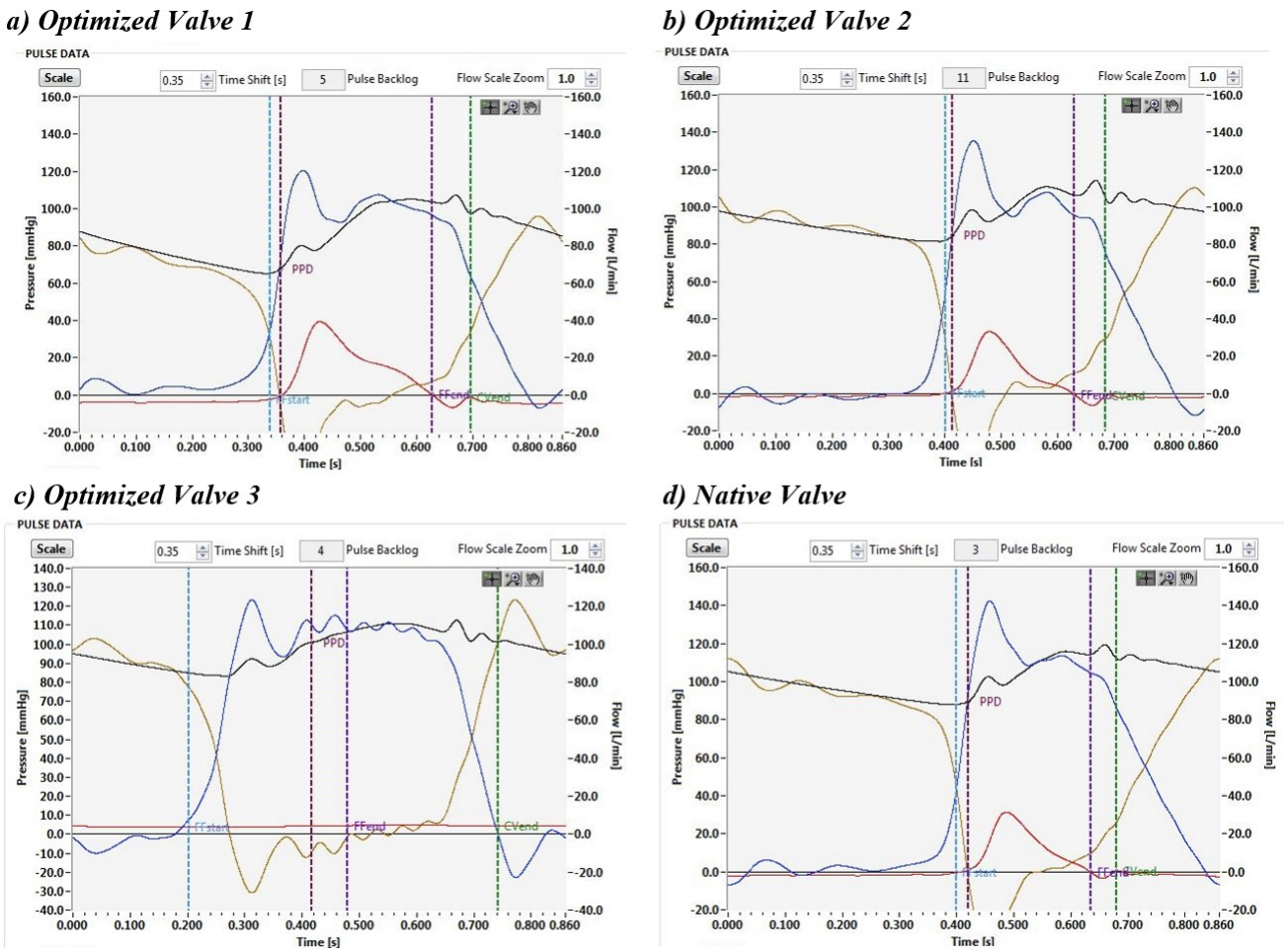

Figure 9. The graphs produced from the pulse duplicator test for each TAV are shown above. These represent various changes in pressure and flow over time during the testing cycles. Maroon represents the positive pressure difference (mmHg), purple represent the forward flow end (L/min), light blue is forward flow start (L/min), green is closing volume end (L/min), dark blue is inflow pressure (mmHg), black is outflow pressure (mmHg), red is flow (L/min), and yellow is pressure difference (mmHg).

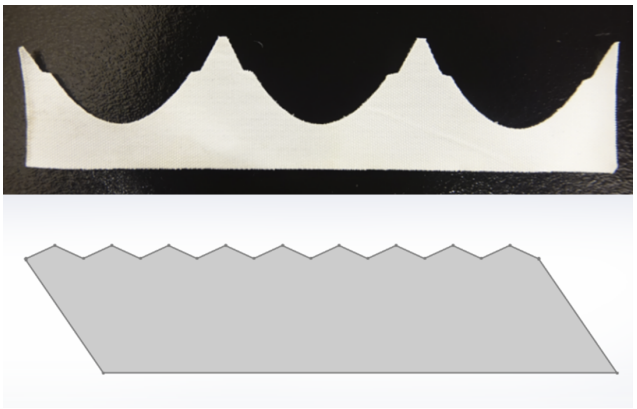

Figure 10. The inner (top) and outer (bottom) Dacron designs are different due to their location in the valve. The outer Dacron is sandwiched between the stent and outer side of the leaflets and matches the stent geometry. The inner Dacron lies within the inner side of the leaflets and matches the leaflet geometry

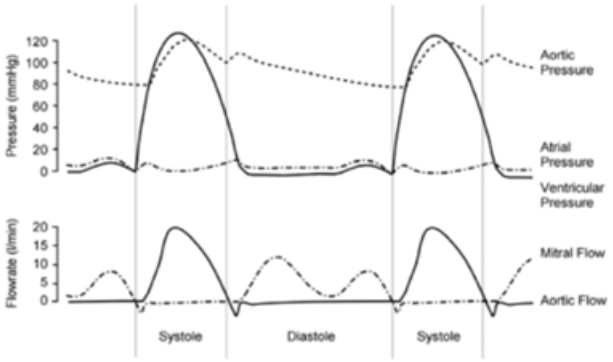

Figure 11. Shown here is a Wiggers Diagram[28]. This represents the various events that occur during a cardiac cycle. These include systole and diastole.

a lower PPD mean than both the native valve and the first optimized valve (Table 2). Furthermore, the second

	PPD Mean (mmHg)	RMS F. Flow (mL/s)	Effective Orifice Area (cm^2)	Total Regurgitation Volume (mL)
Optimized Valve #1	17.378 (*SD = 0.853*)	359.41 (*SD = –5.78*)	1.7560 (*SD = 0.0513*)	–41.164 (*SD = 1.49*)
Optimized Valve #2	14.585 (*SD = 0.962*)	290.77 (*SD = 3.20*)	1.5516 (*SD = 0.046*)	–20.212 (*SD = 2.13*)
Native Valve	16.550 (*SD = 0.518*)	277.74 (*SD = 2.56*)	1.3898 (*SD = 0.023*)	–18.345 (*SD = –1.79*)

Table 2 Calculated data for each TAV. The average value over an average of 10 cycles is shown for each valve. Underneath this average is a standard deviation for the data collected over the ten cycles. The included valves are the first two optimized valves and the native valve. While the third optimized valve was unable to produce quality data for all calculations, the PPD mean and regurgitation values of the second optimized valve are approximated to be the same for the third optimized valve. The flow of the pulse duplicator was set at a cardiac output of 5 L/min.

optimized valve had a higher effective orifice area than the native valve (Table 2). This shows that the second optimized valve performed better during the systolic period of the cycles. However, the native valve can reject the hypothesis through the analysis of the diastole conditions. The native valve had the lowest total regurgitation volume during the diastole period (Table 2). Lower regurgitation values are preferential for a patient's health. The second optimized TAV however still has a lower regurgitation value than the first optimized TAV, showing that the design for the optimized TAV's improved in diastole as well as systole

Both the optimized valve and native valve used similar methods for their Dacron's, stents, and leaflets, but had core differences in their design such as values for H, R_b, R_c, α, and θ. The native valve had a shorter height, a matching R_b and R_c, a lower value for α, and a higher value for θ. It was hypothesized that the best optimized design would behave better than the native design because it was designed to account for various changes such as the material from a natural aortic valve to a manufactured TAV. While this was supported during systole, the native valve was superior during diastole. All the valves performed moderately well, even though some were better than others. They all had low standard deviation values per cycle for PPD mean, RMS F. Flow, effective orifice area, and regurgitation volume. This shows that they were able to continually perform under the harsh conditions of the pulse duplicator, without deforming shape or loosing quality. During this experiment it was seen that a diamond geometry is preferential to a quadrilateral geometry for the stents. Finally, an inner Dacron, running sutures, and tough resin material are crucial for a high valve performance as well.

5 FURTHER DIRECTIONS

Future projects will continue to focus on altering designs of TAVs to be just as, if not more, durable than SAVs. This experiment had some issues that can be improved upon in the future. A main problem from this experiment was the regurgitation through the valve during diastole. This occurred through gaps between the leaflets as well as between the leaflets and frame/Dacron component. In future experiments, this can be minimized by increasing the number of stitches, using blood instead of the glycerin/saline solution, and redesigning the stent. In addition, the third optimized valve failed. This can be rectified with an improved calibration method for the pulse duplicator. Furthermore, this experiment used a rigid stent as opposed to a collapsible stent, due to limited time and the desire to focus primarily on leaflet function and basic stent geometry. A similar study in the future could focus on a collapsible alloy stents, as most TAV studies do. The results of this study and other data available in the literature underline the opportunity to improve leaflet design in the next generation of TAVs to increase long-term durability of transcatheter heart valves.

6 ACKNOWLEDGEMENTS

This research was completed at the University of Denver in the Cardiovascular Biomechanics Laboratory [29], and supported by the university's Undergraduate Research Center's Summer Research Grant. The award number was PinS 84870 [30]. The Principal Investigator of this study was Samantha Shoun and the professor mentoring and guiding her was Dr. Ali Azadani. Other lab members including Dong Qiu and Mina Shafiei heavily assisted with testing, designing, and data analysis. In addition, Justin Huff assisted with the resin printing of the stents. This work could not have been completed without the amazing team at DU Biomechanics Cardiovascular Lab.

7 EDITOR'S NOTES

This article was peer-reviewed.

REFERENCES

[1] Iung, B. *et al.* A prospective survey of patients with valvular heart disease in Europe: The Euro Heart Survey on Valvular Heart Disease. *European Heart Journal* **24**, 1231–1243 (2003).

[2] Nkomo, V. T. *et al.* Burden of valvular heart diseases: a population-based study. *The Lancet* **368**, 1005–1011 (2006).

[3] Takkenberg, J. J. M. *et al.* The need for a global perspective on heart valve disease epidemiology: The SHVD working group on epidemiology of heart valve disease founding statement. *The Journal of Heart Valve Disease* **17**, 135–139 (2008).

[4] Yacoub, M. H. & Takkenberg, J. J. M. Will heart valve tissue engineering change the world? *Nature Clinical Practice: Cardiovascular Medicine* **2**, 60–61 (2005).

[5] De Santo, L. S. *et al.* Mechanical aortic valve replacement in young women planning on pregnancy: maternal and fetal outcomes under low oral anticoagulation, a pilot observational study on a comprehensive pre-operative counseling protocol. *Journal of the American College of Cardiology* **59**, 1110–1115 (2012).

[6] Adams, D. H., Popma, J. J. & Reardon, M. J. Transcatheter aortic-valve replacement with a self-expanding prosthesis. *The New England Journal of Medicine* **371**, 967–968 (2014).

[7] Smith, C. R. *et al.* Transcatheter versus surgical aortic-valve replacement in high-risk patients. *The New England Journal of Medicine* **364**, 2187–2198 (2011).

[8] Leon, M. B. *et al.* Transcatheter or Surgical Aortic-Valve Replacement in Intermediate-Risk Patients. *The New England Journal of Medicine* **374**, 1609–1620 (2016).

[9] Mack, M. J. *et al.* Transcatheter Aortic-Valve Replacement with a Balloon-Expandable Valve in Low-Risk Patients. *The New England Journal of Medicine* **380**, 1695–1705 (2019).

[10] Antelope Valley Hospital. TAVR (2022). URL https://www.avmc.org/news/press-release/2021/taking-care-of-antelope-valley-hearts-for-heart-/.

[11] Arsalan, M. & Walther, T. Durability of prostheses for transcatheter aortic valve implantation. *Nature Reviews: Cardiology* **13**, 360–367 (2016).

[12] Dvir, D. E. H. *et al.* First Look at Long-Term Durability of Transcatheter Heart Valves: Assessment of Valve Function up to 10 Years After Implementation (2016).

[13] Bourguignon, T. *et al.* Very long-term outcomes of the Carpentier-Edwards Perimount valve in aortic position. *The Annals of Thoracic Surgery* **99**, 831–837 (2015).

[14] Grunkemeier, G. L., Furnary, A. P., Wu, Y., Wang, L. & Starr, A. Durability of pericardial versus porcine bioprosthetic heart valves. *The Journal of Thoracic and Cardiovascular Surgery* **144**, 1381–1386 (2012).

[15] Johnston, D. R. *et al.* Long-term durability of bioprosthetic aortic valves: implications from 12,569 implants. *The Annals of Thoracic Surgery* **99**, 1239–1247 (2015).

[16] Rodriguez-Gabella, T., Voisine, P., Puri, R., Pibarot, P. & Rodés-Cabau, J. Aortic Bioprosthetic Valve Durability: Incidence, Mechanisms, Predictors, and Management of Surgical and Transcatheter Valve Degeneration. *Journal of the American College of Cardiology* **70**, 1013–1028 (2017).

[17] Schoen, F. J. & Levy, R. J. Calcification of tissue heart valve substitutes: progress toward understanding and prevention. *The Annals of Thoracic Surgery* **79**, 1072–1080 (2005).

[18] Thubrikar, M. J. *The Aortic Valve* (2011).

[19] Edwards Lifesciences Corporation. European Patent Specification (2020).

[20] Abbasi, M. & Azadani, A. N. A geometry optimization framework for transcatheter heart valve leaflet design. *Journal of the Mechanical Behavior of Biomedical Materials* **102**, 103491 (2020).

[21] Kerr, M. M. & Gourlay, T. Design and numerical simulation for the development of an expandable paediatric heart valve. *The International Journal of Artificial Organs* **44**, 518–524 (2021).

[22] EpilogLaser. The Fusion Laser Series by Epilog Laser: Laser Engraving and Cutting Systems (2022). URL wwwepiloglaser.com.

[23] Formlabs. Form 2: Affordable Desktop SLA 3D Printer. URL https://formlabs.com/3d-printers/form-2/.

[24] Abbasi, M., Barakat, M. S., Dvir, D. & Azadani, A. N. A Non-Invasive Material Characterization Framework for Bioprosthetic Heart Valves. *Annals of biomedical engineering* **47**, 97–112 (2019).

[25] BDC Laboratories. BDC Laboratories PD-1100 System User Guide (2017).

[26] Zuhdi, N. *et al.* Porcine aortic valves as replacements for human heart valves. *The Annals of Thoracic Surgery* **17**, 479–491 (1974).

[27] Garcia, D. *et al.* Estimation of aortic valve effective orifice area by Doppler echocardiography: effects of valve inflow shape and flow rate. *Journal of the American Society of Echocardiography* **17**, 756–765 (2004).

[28] ISO. Cardiovascular implants — Cardiac valve prostheses — Part 1: General requirements (2022).

URL https://www.iso.org/obp/ui/#iso:std:iso:5840:-1:ed-1:v1:en:term:3.19.

[29] University of Denver. Cardiovascular Biomechanics | Engineering & Computer Science (2022). URL ritchieschool.du.edu.

[30] University of Denver. Funding | Undergraduate Research Center (2022). URL www.du.edu.